Influence of the Film Thickness and Morphology on the Colorimetric Properties of Spray-Coated Electrochromic Disubstituted 3,4-Propylenedioxythiophene Polymers

Roger J. Mortimer,* Kenneth R. Graham, Christophe R. G. Grenier, and John R. Reynolds

The George and Josephine Butler Polymer Research Laboratory, Department of Chemistry, Center for Macromolecular Science and Engineering, University of Florida, Gainesville, Florida 32611-7200

ABSTRACT Variation of the colorimetric properties as a function of the film thickness and morphology has been investigated for two spray-coated electrochromic disubstituted 3,4-propylenedioxythiophene polymers. Changes in the luminance, hue, and saturation have been tracked using CIE 1931 *Lxy* chromaticity coordinates, with CIELAB 1976 color space coordinates, L^*, a^*, and b^*, being used to quantify the colors. For (precycled) neutral PProDOT-$(Hx)_2$ films, with an increase in the thickness, L^* is seen to decrease, with a^* and b^* coordinates moving in positive and negative directions, respectively, with quantification of the pink/purple (magenta) color as the summation of red and blue. For all thicknesses, L^* is comparable, pre- and postcycling, with a^* decreasing (less red) and b^* becoming more negative (more blue) and the film now appearing as purple in the neutral state. Color coordinates for the reverse (reduction) direction exhibited hysteresis in comparison with the initial oxidation, with the specific choice of perceived color values depending not only on the film thickness but also on both the potential applied and from which direction the potential is changed. Neutral PProDOT-$(2\text{-MeBu})_2$ films appear blue/purple to the eye both as-deposited and after potential cycling to the transparent oxidized state. For the neutral, colored state, with an increase in the thickness, L^* is seen to decrease, with a^* and b^* coordinates moving in positive and negative directions, respectively. For PProDOT-$(2\text{-MeBu})_2$ films, the a^* coordinates are lower positive values and the b^* coordinates are higher negative values, thus quantifying the high dominance of the blue color in the blue/purple films compared to the pink/purple PProDOT-$(Hx)_2$ films. As for the PProDOT-$(Hx)_2$ films, the tracks of the color coordinates show that the specific choice of perceived color values depends on the film thickness. Unlike the PProDOT-$(Hx)_2$ films, hysteresis is absent in the oxidation/reduction track of the $x-y$ coordinates for the PProDOT-$(2\text{-MeBu})_2$ films, although slight hysteresis is present in the luminance. Characterization of the film morphologies through atomic force microscopy reveals a much rougher, higher surface area morphology for the PProDOT-$(2\text{-MeBu})_2$ films versus the PProDOT-$(Hx)_2$ films. The branched repeat unit in the PProDOT-$(2\text{-MeBu})_2$ films provides a structure that allows ions to ingress/egress more effectively, thus removing hysteresis from the optical response.

KEYWORDS: electrochromism • electrochromic • colorimetry • conjugated conducting polymer • morphology • spray-cast films

INTRODUCTION

Electrochromism is a change, evocation, or bleaching of color as effected either by an electron-transfer (redox) process or by a sufficient electric potential (1). Visible electrochromism is useful for display purposes if one of the colors is markedly different from the other, such as, for example, when the absorption band of one redox state is in the visible region of the electromagnetic spectrum, while the other is in the ultraviolet (UV). If the colors are sufficiently intense and different, then the material is said to be electrochromic and the species undergoing change is usefully termed an "electrochrome" (1).

Conjugated conducting polymers receive particular attention for their potential use in controllable light-reflective or light-transmissive electrochromic displays for optical information and storage (2, 3). They have fast switching speeds, high contrast ratios, and high coloration efficiencies. Several are available as solution-processable materials, and their electrochromic properties and color states can be synthetically tuned (4). In the oxidized state, conjugated conducting polymers are charge-balanced, "doped", with counteranions ("p-doping") and have a delocalized π-electron band structure (5). The reduction of "p-doped" conjugated conducting polymers, with a concurrent counteranion exit (or electrolyte cation incorporation), yields the "undoped" (neutral) electrically insulating form. The electronic band gap (E_g), defined as the energy difference between the highest occupied π-electron band (valence band) and the lowest unoccupied band (the conduction band), determines the intrinsic optical properties. The color change or contrast between doped and undoped forms of the polymer depends on the magnitude of the band gap of the undoped polymer. Thin films of conjugated conducting polymers with E_g greater than 3 eV (~400 nm) are colorless and transparent in the undoped form, while in the doped form, they generally absorb visible radiation. Those with E_g equal to or less than 1.8–1.9 eV (~650–700 nm) tend to be highly absorbing in the undoped form, but after doping, the free carrier absorption is relatively weak in the visible region because it is transferred to

* Permanent address: Department of Chemistry, Loughborough University, Loughborough, Leicestershire LE11 3TU, U.K. E-mail: R.J.Mortimer@lboro.ac.uk. Tel: +44 1509 222583. Fax: +44 1509 223925.

Received for review June 21, 2009 and accepted September 11, 2009

DOI: 10.1021/am900431z

the near-infrared (NIR). Polymers with intermediate gaps have distinct optical changes throughout the visible region and can exhibit several colors. Through band-gap control, achieved primarily through main-chain and pendant group structural modification, the accessible color states in both the doped (conductive) and neutral (insulating) forms of a conjugated conducting polymer can be varied (4), with both cathodically and anodically coloring electrochromes being available.

Color (6, 7) is a subjective phenomenon, causing the description of the color difference or the comparison of two colors to be quite difficult. However, much effort has been given to the development of *colorimetric analysis*, which allows a quantitative description of the color and relative transmissivity as perceived by the human eye. Colorimetry provides a more precise way to define color than spectrophotometry (8). Rather than record absorption bands, in colorimetry the human eye's sensitivity to light across the visible region is measured and a numerical description of the color is given. There are three attributes that are used to describe the color. The first identifies a color by its location in the spectral sequence, i.e., what wavelength is associated with the color. This is known as the hue, dominant wavelength, or chromatic color and is the wavelength where maximum contrast occurs. It is this aspect that is commonly, but mistakenly, referred to as color. The second attribute, relating to the level of white and/or black, is known as saturation, chroma, tone, intensity, or purity. The third attribute is the brightness of the color, also referred to as value, lightness, or luminance. Luminance is very informative in considering the properties of electrochromes because, with only one value, it provides information about the perceived transparency of a sample over the entire visible range. Since the introduction (9) of a simple in situ colorimetric analysis method for the precise control and measurement of the color in electrochromic systems, this approach has been successfully applied to the characterization of numerous electrochromic conjugated polymer films and display devices prepared therefrom (10) and more recently to nickel oxide with various metal additives (11), thin films of the intervalence charge-transfer complex Prussian blue [iron(III) hexacyanoferrate(II)] (12), and electrochromism in the di-*n*-heptylviologen system (13). Throughout all of these colorimetry studies, the thickness of the electrochromic film has generally been optimized to give the best contrast ratio for color switching and the morphology of the films has largely been neglected. We now report a study of the perceived color of electrochromic conjugated conducting polymer films, with variation of the thickness, and the morphology characterization of these films. Soluble, solution-processable disubstituted poly(3,4-propylenedioxythiophene) (PProDOT) polymers (14) were chosen for the investigation, with the film thickness being varied through the spray-coating deposition time and the morphologies probed through atomic force microscopy (AFM).

RESULTS AND DISCUSSION

Morphology of the PProDOT-(Hx)$_2$ and PProDOT-(2-MeBu)$_2$ Films. Polymer films were spray-cast onto tin-doped indium oxide (ITO)-coated glass at room temperature from toluene. Spray-coated deposits appear uniform to the eye and display excellent contrast on electrochromic color switching. However, upon observation with an optical microscope and an atomic force microscope, it becomes apparent that the films are not uniform on a micrometer length scale, as is evident in Figure 1. To gain a more complete picture of the film morphologies, several

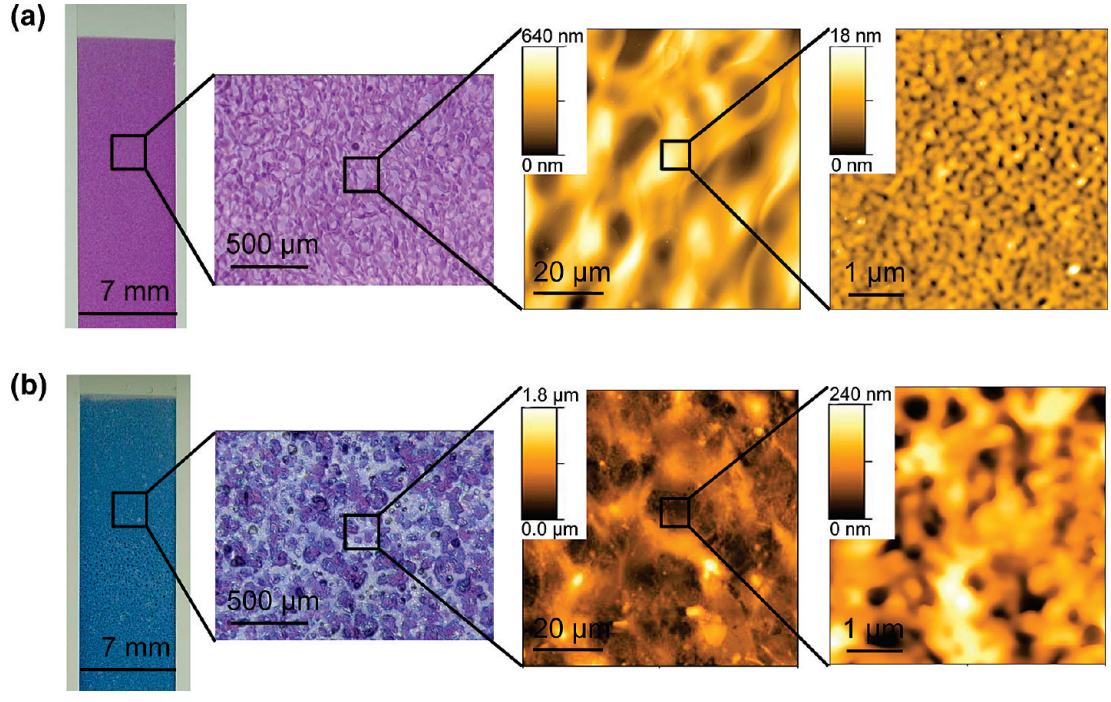

FIGURE 1. Film appearance and morphology as the image size is reduced from a standard photograph to an optical micrograph and to large- and small-scale AFM images (from left to right) of (a) PProDOT-(Hx)$_2$ and (b) PProDOT-(2-MeBu)$_2$ films with absorbance maxima of ~1.0. Note that the color of the AFM images corresponds to the film height and not the true film color.

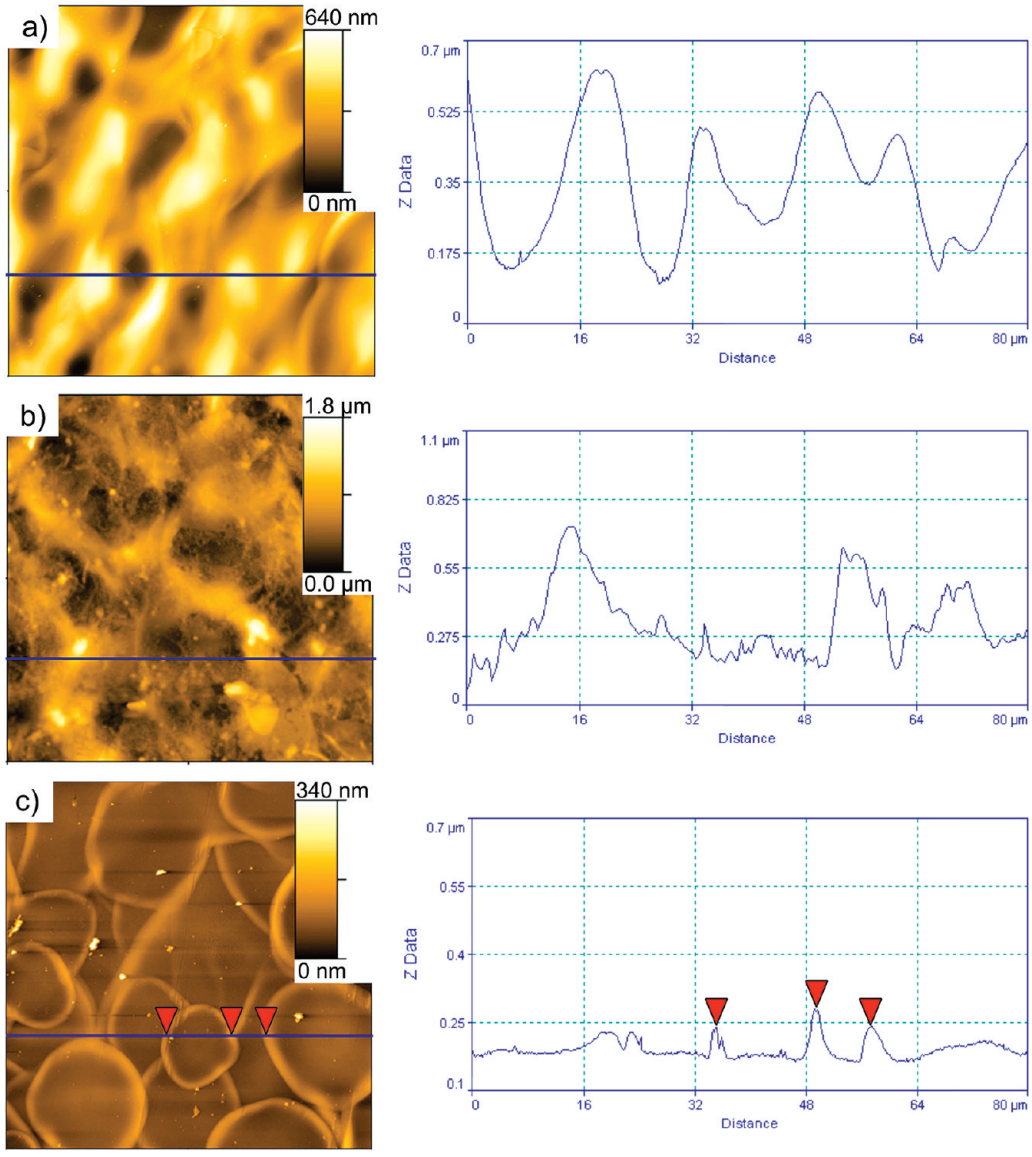

FIGURE 2. AFM height images and the corresponding line traces for (a) a PProDOT-$(Hx)_2$ film with an absorbance of 0.96 (554 nm), (b) a PProDOT-$(2\text{-MeBu})_2$ film with an absorbance of 0.99 (624 nm), and (c) a thinner PProDOT-$(Hx)_2$ film with an absorbance of 0.17 (554 nm). The thinner PProDOT-$(Hx)_2$ film (c) shows evidence of solvent droplet evaporation, with the edges of the droplets indicated by the red triangles. All images are 80 × 80 μm.

PProDOT-$(Hx)_2$ and PProDOT-$(2\text{-MeBu})_2$ films of varying thicknesses were examined by AFM at large (80 μm) and relatively small (5 μm) scan areas. Figure 1 highlights changes in the film appearance and morphology as the field of view is decreased from a photograph to a 5 × 5 μm AFM image.

The color and the morphologies of the PProDOT-$(Hx)_2$ and PProDOT-$(2\text{-MeBu})_2$ films are distinctly different at all length scales. The morphologies of the PProDOT-$(Hx)_2$ deposits are found to vary in accordance with the film thickness. In the thicker samples, there is a fairly smooth undulating morphology with peaks and valleys differing in height by 300−500 nm, as is evident in Figure 2a. As the PProDOT-$(Hx)_2$ films become thinner, an underlying 30−50 nm film, with uneven polymer deposits on top and clear evidence of droplet evaporation, becomes apparent, as shown in Figure 2c. In both thin and thick films, the morphology appears relatively smooth, with more gentle sloping features present.

In contrast, PProDOT-$(2\text{-MeBu})_2$ films were much more patchy, with large aggregates occurring in places such as those evident in Figure 2b. The morphologies were also much more jagged, with sharper peaks and a lack of the smooth undulating morphology seen in the PProDOT-$(Hx)_2$ films. The thinner PProDOT-$(2\text{-MeBu})_2$ films also showed large aggregates and a rougher morphology than the comparably thick PProDOT-$(Hx)_2$ films. The evidence of droplet evaporation apparent in the thinner PProDOT-$(Hx)_2$ films (Figure 2c) is not present in the thinner PProDOT-$(2\text{-MeBu})_2$ films. This morphology presumably originates from the poorer solubility of this polymer and explains the need for multiple coatings necessary to obtain appreciable "thicknesses"/absorbances. With both PProDOT derivatives, there is a significant difference in the morphology of the thinner and thicker films, as is evident in Figure 2.

The morphology of the films was also studied on a smaller scale. The smaller-scale images display an underlying mor-

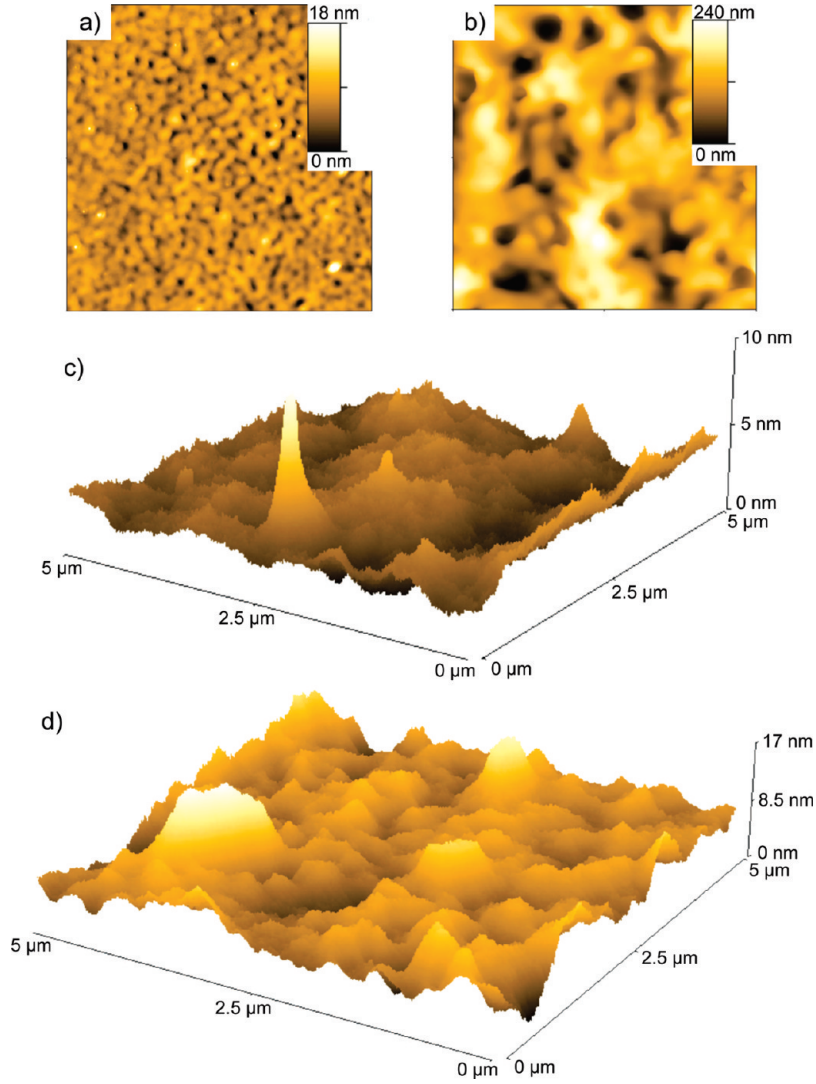

FIGURE 3. AFM height images for (a) a PProDOT-(Hx)$_2$ film with an absorbance of 0.96 (554 nm) and (b) a PProDOT-(2-MeBu)$_2$ film with an absorbance of 0.99 (624 nm). Also shown are (c) three-dimensional AFM height images of a thinner PProDOT-(Hx)$_2$ film with an absorbance of 0.42 (554 nm) and (d) a PProDOT-(2-MeBu)$_2$ film with an absorbance of 0.37 (624 nm). All images are 5 × 5 μm. Note that the scale bars on images c and d are 10 and 17 nm, respectively.

phology that is almost completely overshadowed by the large height variations in the larger-scale images. All 5 × 5 μm areas were selected by first scanning a 20 × 20 μm area and then selecting and scanning the smoothest 5 × 5 μm area; therefore, the small scans are generally aggregate-free regions in the middle of the dried droplets. The PProDOT-(Hx)$_2$ films show a fairly uniform and smooth morphology in a 5 μm × 5 μm area (Figure 3a,c) with root-mean-square (rms) surface roughnesses generally in the 1−2 nm range. As may be expected, the morphology of the thicker films had a slightly higher surface roughness with more features present. The PProDOT-(2-MeBu)$_2$ films show a much rougher and more porous morphology, as is evident in Figure 3b,d. This rougher morphology becomes especially apparent in the thicker films, with the thickest film displaying an rms surface roughness of 44 nm, as shown in Figure 3b. Note that in Figure 3a the height scale for the PProDOT-(Hx)$_2$ film is 18 nm, whereas the height scale for the PProDOT-(2-MeBu)$_2$ film in Figure 3b is 240 nm. The thinner PProDOT-(2-MeBu)$_2$ films have a much smoother morphology than the thickest film; however, they generally have rms surface roughnesses of approximately 2−3 times larger than the comparably thick PProDOT-(Hx)$_2$ films.

Colorimetry of PProDOT-(Hx)$_2$ Films. The polymer film thickness, as indicated by the absorbance at λ_{max} and the electrochemical switching charge in the supporting electrolyte solution (0.1 M lithium perchlorate in propylene carbonate), was controlled by the spray-casting deposition time. Data for three representative thicknesses are given in Table 1, which shows CIE (Commission Internationale de l'Eclairage) 1931 colorimetric luminance (%Y), x−y coordinates, and the resulting calculated CIELAB $L^*a^*b^*$ coordinates for the as-deposited neutral pink/purple (magenta) films in 0.1 M lithium perchlorate/propylene carbonate at an open circuit and following conditioning by potential cycling (10 cycles between 0.000 and +0.900 V vs Ag wire at 100 mV s^{-1}) to the very pale gray/green oxidized state. The CIELAB $L^*a^*b^*$ coordinates are a uniform color space defined by CIE in 1976 and offer a standard commonly used

Table 1. Colorimetric, Spectrophotometric, and Electrochemical Data for Three PProDOT-$(Hx)_2$ Films of Increasing Thickness on ITO/Glass Substrates in 0.1 M Lithium Perchlorate/Propylene Carbonate[a]

	% *L*	*x*	*y*	*L**	*a**	*b**	color by the eye	*A* (at 554 nm)	*Q* (mC cm^{-2})
b	71.3	0.359	0.360	88	10	−12	pink/purple		
c	68.1	0.355	0.359	86	9	−13	purple	0.17	0.1
b	36.7	0.373	0.323	67	27	−19	pink/purple		
c	32.4	0.350	0.313	64	22	−25	purple	0.42	0.3
b	15.3	0.399	0.270	46	45	−25	pink/purple		
c	11.4	0.330	0.239	40	34	−39	purple	0.96	1.0

[a] *A* is the absorbance at λ_{max} of the polymer. The switching charge, *Q*, was measured by current integration following a potential step between the neutral and oxidized states. [b] Colorimetric data measured at an open circuit for the as-deposited neutral state. [c] Colorimetric data measured at an open circuit for the neutral state, following potential cycling (10 cycles between 0.000 and +0.900 V vs Ag wire at 100 mV s^{-1}) between the neutral and oxidized states.

in the paint, plastic, and textile industries. *L** is the lightness variable of the sample, while *a** and *b** correspond to the two antagonistic chromatic processes (red-green and yellow-blue). In the *L***a***b** chromaticity diagram, +*a** is the red direction, −*a** is the green direction, +*b** is the yellow direction, and −*b** is the blue direction. The center (0, 0) of the chromaticity diagram is achromatic; as the *a** and *b** values increase, the saturation of the color increases.

For the precycled films (Table 1), with an increase in the thickness, the luminance *L** is seen to decrease, with *a** and *b** coordinates moving in positive and negative directions, respectively, thus quantifying the increasingly saturated pink/purple (magenta) color as the summation of red and blue. The perceived color therefore varies with the thickness, and to reproduce a film of given color coordinates, it is essential to prepare the same thickness.

Upon potential cycling of the (initially) neutral PProDOT-$(Hx)_2$ films to the very pale gray/green oxidized state, following the first cycle, the initially pink/purple (magenta) film transforms to purple back at 0.000 V, with quantification of this (postcycling) different color given in Table 1. For all thicknesses, *L** is comparable, pre- and postcycling, with *a** decreasing (less red) and *b** becoming more negative (more blue) and the film now appearing as purple in the neutral state.

In situ colorimetric measurements were next recorded as a function of the film thickness, as the potential was slowly stepped, in 0.050 V intervals, in sequence over the range 0.000 to +0.900 V, and then in reverse. For the three representative thicknesses, Figure 4a shows colorimetric luminance (% *L*), at each applied potential, and the calculated *L***a***b** coordinates for each neutral and oxidized state at the two potential limits. Figure 5 shows *x*−*y* coordinates at each applied potential for the three thicknesses. Tables S1−S3 (in the Supporting Information) show full colorimetric data at each applied potential. Upon film oxidation, the *L***a***b** coordinates quantify the bleaching of the color and the increase in transmissivity. For the thinnest film, the tint of the oxidized form is imperceptible by the human eye, with the *L***a***b** coordinates (97, 0, 0) very nearly reaching the achromatic "white point" of the color space. Color coordinates for the reverse (reduction) direction plots (Figures 4a and 5) show hysteresis in comparison with the initial oxidation sequence, implying that the specific choice of perceived color values depends not only on the film thickness but also on both the potential applied and from which direction the potential is changed.

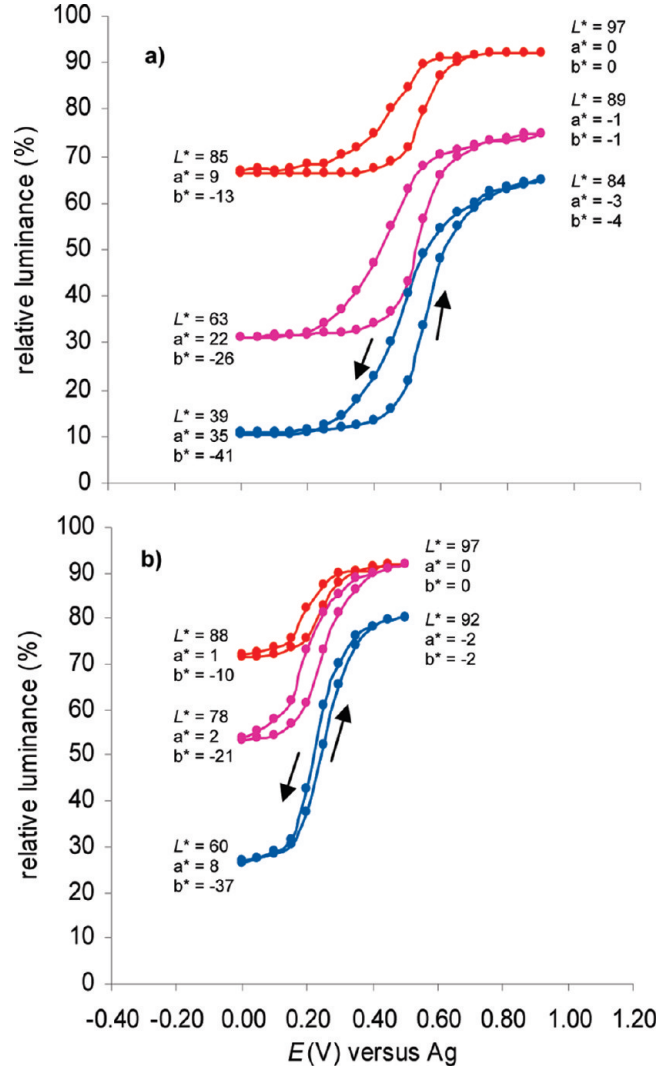

FIGURE 4. Relative luminance as a function of the applied potential and film thickness for spray-coated (a) PProDOT-$(Hx)_2$ and (b) PProDOT-$(2\text{-MeBu})_2$. Absorbances of the deposited neutral films (estimated at the absorption maximum) give an indication of the thickness obtained upon spraying and were 0.17 (red line), 0.42 (pink line), and 0.96 (blue line) (at 554 nm) for part a and 0.18 (red line), 0.37 (pink line), and 0.99 (blue line) (at 624 nm) for part b. For color matching, *L*a***b** values of fully neutral and oxidized states are given for the films.**

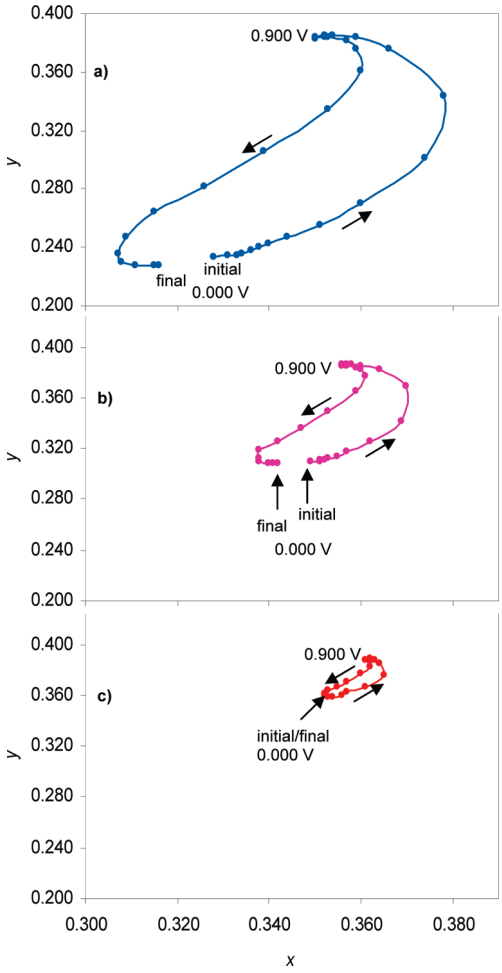

FIGURE 5. CIE 1931 $x-y$ chromaticity data as a function of the applied potential and film thickness for spray-coated PProDOT-$(Hx)_2$ (a–c). Absorbances of the neutral deposited film were (a) 0.96 (at 554 nm), (b) 0.42 (at 554 nm), and (c) 0.17 (at 554 nm). The potential (E/V vs Ag wire) was increased in 0.050 V intervals from the initial neutral form at 0.000 V to the oxidized form at +0.900 V and then in reverse. The initial and final $x-y$ coordinates at 0.000 V, the coordinates at +0.900 V, and the direction of the track of the color locus are all indicated.

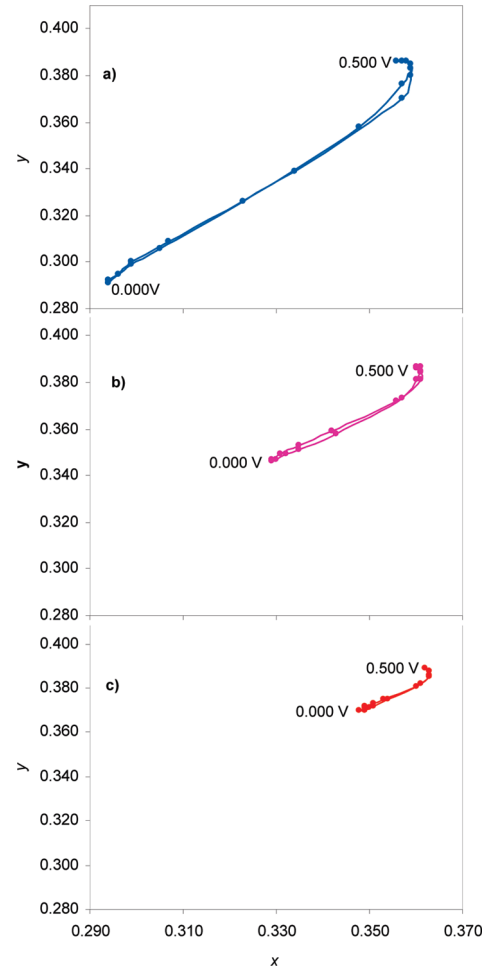

FIGURE 6. CIE 1931 $x-y$ chromaticity data as a function of the applied potential and film thickness for spray-coated PProDOT-(2-MeBu)$_2$(a–c). Absorbances of the neutral deposited film were (a) 0.99 (at 624 nm), (b) 0.37 (at 624 nm), and (c) 0.18 (at 624 nm). The potential (E/V vs Ag wire) was increased in 0.050 V intervals from the initial neutral form at 0.000 V to the oxidized form at +0.500 V and then in reverse. The initial and final $x-y$ coordinates at 0.000 V and the coordinates at +0.500 V are indicated.

Colorimetry of PProDOT-(2-MeBu)$_2$ Films. Neutral PProDOT-(2-MeBu)$_2$ films appear blue/purple to the human eye both as-deposited and after potential cycling to the transparent oxidized state. In situ colorimetric measurements were recorded as a function of the PProDOT-(2-MeBu)$_2$ film thickness, following potential cycling, as the potential is slowly stepped, in 0.050 V intervals, in sequence over the range 0.000 to +0.500 V, and then in reverse. For three representative thicknesses, Figure 4b shows colorimetric luminance (% L), at each applied potential, and the calculated $L^*a^*b^*$ coordinates for each neutral and oxidized state at the two potential limits. For all three thicknesses, the tint of the oxidized form is imperceptible to the human eye, with the $L^*a^*b^*$ coordinates (97, 0, 0) and (92, −2, −2) very nearly reaching the achromatic "white point" of the color space. Figure 6 shows $x-y$ coordinates at each applied potential. Tables S4–S6 (in the Supporting Information) show full colorimetric data at each applied potential. Upon film oxidation, the $L^*a^*b^*$ coordinates quantify the bleaching of the color and the increase in transmissivity. For the neutral, colored state (at 0.000 V), with an increase in the thickness, L^* is seen to decrease, with a^* and b^* coordinates moving in positive and negative directions, respectively, thus quantifying the increasingly saturated color. For PProDOT-(2-MeBu)$_2$ films, the a^* coordinates are low positive values and the b^* coordinates are higher negative values, owing to the dominance of the blue color in the blue/purple films compared to the pink/purple PProDOT-$(Hx)_2$ films.

As for the PProDOT-$(Hx)_2$ films, the tracks of the color coordinates show that the specific choice of perceived color values depends on the film thickness. Unlike the PProDOT-$(Hx)_2$ films, hysteresis is absent in the oxidation/reduction track of the $x-y$ coordinates for the PProDOT-(2-MeBu)$_2$ films. A comparison of parts a and b of Figure 4 shows the PProDOT-(2-MeBu)$_2$ films to switch color over a shorter potential interval, with only slight hysteresis. The branched repeat unit provides a structure that allows ions to ingress/egress more effectively, leading to the lack of hysteresis evident in the colorimetric data of the PProDOT-(2-MeBu)$_2$ films. The smoother PProDOT-$(Hx)_2$ films have less exposed surface area, and therefore the electrolyte penetration is

much slower. This slower electrolyte penetration likely contributes to the hysteresis evident in colorimetric data of the PProDOT-$(Hx)_2$ films.

CONCLUSION

A colorimetric method, based on the CIE system of colorimetry, has been used to study variation of the perceived color as a function of the film thickness and morphology for two spray-coated electrochromic disubstituted 3,4-propylenedioxythiophene polymers on transmissive ITO/glass substrates. The technique is a convenient method for the precise measurement of the hue, saturation, and luminance of the color states and allows the changes in these properties to be carefully monitored on redox switching between electrochromic color states. The perceived colors vary with the thickness, and therefore to reproduce a film of given color coordinates, it is essential to prepare the same thickness of a given polymer. For PProDOT-$(Hx)_2$ films, color coordinates for the reverse (reduction) direction plots show hysteresis upon comparison with the initial oxidation, implying that the specific choice of perceived color values depends not only on the film thickness but also on both the potential applied and from which direction the potential is changed. This observed hysteresis in the PProDOT-$(Hx)_2$ films is attributed, in part, to the smoother, lower surface area morphology. The minimal hysteresis observed in the PProDOT-$(2\text{-MeBu})_2$ films suggests that the dopant anions move in and out of the films more readily. A rougher, higher surface area morphology is observed for the PProDOT-$(2\text{-MeBu})_2$ films and is likely due to a reduced solubility of this polymer relative to PProDOT-$(Hx)_2$, leading to more rapid precipitation during the spray-coating process.

EXPERIMENTAL SECTION

Materials, Film Formation, and Characterization. Working electrode substrates were tin-doped indium oxide (ITO) on glass ($7 \times 50 \times 0.7$ mm, 5−15 Ω/□, part number CG-50IN-CUV) from Delta Technologies Limited. Before use, the ITO/glass substrates were rinsed in acetone, in order to remove any trace of adhesive/impurities on the surface, followed by rinsing with deionized water and air drying. PProDOT-$(Hx)_2$ [poly(3,3-dihexyl-3,4-dihydro-2*H*-thieno[3,4-*b*][1,4]dioxepine), black solid flakes] and racemic PProDOT-$(2\text{-MeBu})_2$ [poly(3,3-bis(2-methylbutyl)-3,4-dihydro-2*H*-thieno[3,4-*b*][1,4]dioxepine), golden, iridescent flakes] were synthesized as previously described (14). For PProDOT-$(Hx)_2$, 4 mL of a 5 mg/mL toluene (Fisher Certified Reagent) solution was prepared in an amber bottle by magnetically stirring at room temperature for 4 h. PProDOT-$(2\text{-MeBu})_2$ was less soluble, with 20 mg of polymer being dissolved in 30 mL of toluene in an amber bottle, after magnetic stirring overnight at room temperature. Prior to film deposition, polymer solutions were filtered through 0.45 μm Whatman PTFE filters, with a syringe being used to apply pressure to the solution to aid filtration. Polymer films were deposited onto horizontally mounted ITO/glass substrates by spray casting from the deep-purple solutions, using an air brush (Iwata ECL2500 Eclipse BS) at 10 psi at a 45° angle. Following each pass of the air brush, coatings were allowed to dry. Multiple coatings provided the appropriate polymer film thickness/absorbance; a Varian Cary 500 Scan UV−vis−NIR spectrophotometer was used to monitor the polymer film thickness, through absorbance measurement in the transmission mode at each polymer's λ_{max} [554 nm for PProDOT-$(Hx)_2$; ~624 nm for PProDOT-$(2\text{-MeBu})_2$]. AFM measurements were carried out using a Veeco Innova scanning probe microscope in tapping mode with a Nanodrive controller and MikroMasch NSC 15 tapping mode silicon probes with ~300 kHz resonant frequency. The optical microscope on the Veeco Innova was calibrated using a standard silicon calibration grating (Veeco model 498-011-501) and used to take the optical micrographs.

Electrochemistry. Electrochemical measurements were carried out in deoxygenated solutions (purged with pure argon) using an EG&G model PAR 273A potentiostat/galvanostat, under the control of Scribner and Associates Corrware II software. No solution resistance compensation was employed. For all measurements, a standard 1 cm quartz cuvette was used as the electrochemical cell. A machined poly(tetrafluoroethylene) lid allowed the electrochromic polymer/ITO/glass working electrode to be mounted parallel to the optical faces of the cuvette. Additional holes in the lid allowed a platinum-plate counter electrode and a silver wire pseudo reference electrode [+0.491 V against the ferrocene (Fluka)/ferrocinium (Fc/Fc^+) redox couple] to be positioned in the electrolyte solution. For all measurements, the lower 35 mm of each electrochromic polymer/ITO/glass substrate was immersed in the electrolyte solution, providing a submerged geometric electrode active area of 2.5 cm^2. Adhesive copper tape (1131 from 3M) at the top of each ITO/glass substrate provided the means for a uniform electrical contact. The supporting electrolyte used was 0.1 M lithium perchlorate (Aldrich) in propylene carbonate (Acros Organics); reagents were used without further purification.

Colorimetry. In situ colorimetric measurements were obtained using a Minolta CS-100 Chroma Meter and a CIE-recommended normal/normal (0/0) illuminating/viewing geometry for transmittance measurements (15). The calibration of the Chroma Meter was set to the preset mode. The standard illuminant was a D_{50} (5000 K), constant-temperature, daylight-simulating light source in a light booth designed to exclude external light. Background color coordinates of the light source as measured with the Chroma Meter were $x = 0.361$ and $y = 0.388$. For measurements under electrochemical control, prior to each set of measurements, background color coordinates (Y, x, and y values) were taken at an open circuit, using a blank ITO/glass substrate in the standard quartz cuvette containing the electrolyte solution. For measurements involving sequences of applied potentials, to ensure readings had equilibrated, color coordinates were recorded after each potential had been applied for 10 s and the current had decayed to background levels. Additional readings were taken at 20 s, to ensure that the color coordinates had stabilized. For all measurements, the electrochromic polymer/ITO/glass substrate was on the side of the cuvette closest to the light source, with the polymer film facing the Chroma Meter. The Yxy values of the standard illuminant were converted to X_n, Y_n, and Z_n tristimulus values (8), which, in turn, were used with the calculated tristimulus values (X, Y, and Z) of each color state for conversion to CIELAB $L^*a^*b^*$ coordinates. The x and y coordinates were calculated from the XYZ tristimulus values using the formulas $x = X/(X + Y + Z)$ and $y = Y/(X + Y + Z)$.

Acknowledgment. We thank the EPSRC for an Overseas Travel Grant (EP/E000746/1) to R.J.M. and AFOSR (Grant FA9550-09-1-0320) for financial support. K.R.G. acknowledges the University Alumni Awards Program for a fellowship.

Supporting Information Available: Percentage of L, x, y, L^*, a^*, and b^* colorimetric data at each applied potential for the three PProDOT-$(Hx)_2$ film thicknesses, corresponding to % L, x, and y data shown graphically in Figures 4a and 5

(Tables S1−S3) and percentage of L, x, y, L^*, a^*, and b^* colorimetric data at each applied potential for the three PProDOT-(2-MeBu)$_2$ film thicknesses, corresponding to % L, x, and y data shown graphically in Figures 4b and 6 (Tables S4−S6). This material is available free of charge via the Internet at http://pubs.acs.org.

REFERENCES AND NOTES

(1) Monk, P. M. S.; Mortimer, R. J.; Rosseinsky, D. R. *Electrochromism and Electrochromic Devices*; Cambridge University Press: Cambridge, U.K., 2007.

(2) Dyer, A. L.; Reynolds, J. R. In *Handbook of Conducting Polymers*, 3rd ed.; Skotheim, T. A., Reynolds, J. R., Eds.; CRC Press: Boca Raton, FL, 2007; Vol. 1, Chapter 20.

(3) Beaujuge, P. M.; Reynolds, J. R. *Chem. Rev.* 2009. Submitted for publication.

(4) See the reviews: (a) Groenendaal, L.; Jonas, F.; Freitag, D.; Pielartzik, H.; Reynolds, J. R. *Adv. Mater.* **2000**, *7*, 481. (b) Groenendaal, L.; Zotti, G.; Aubert, P.-H.; Waybright, S. M.; Reynolds, J. R. *Adv. Mater.* **2003**, *15*, 855. (c) Argun, A. A.; Aubert, P.-H.; Thompson, B. C.; Schwendeman, I.; Gaupp, C. L.; Hwang, J.; Pinto, N. J.; Tanner, D. B.; MacDiarmid, A. G.; Reynolds, J. R. *Chem. Mater.* **2004**, *16*, 4401. (d) Walczak, R. M.; Reynolds, J. R. *Adv. Mater.* **2006**, *18*, 1121.

(5) Roncali, J. *Chem. Rev.* **1992**, *92*, 711.

(6) Christie, R. M. *Colour Chemistry*; Royal Society of Chemistry: Cambridge, U.K., 2001; Chapter 2.

(7) Kuehni, R. G. *Color: An Introduction to Practice and Principles*, 2nd ed.; John Wiley & Sons, Inc.: Hoboken, NJ, 2005.

(8) Wyszecki, G.; Stiles, W. S. *Color Science: Concepts and Methods, Quantitative Data and Formulae*, 2nd ed.; John Wiley & Sons: New York, 1982.

(9) Thompson, B. C.; Schottland, P.; Zong, K.; Reynolds, J. R. *Chem. Mater.* **2000**, *12*, 1563.

(10) (a) Thompson, B. C.; Schottland, P.; Sönmez, G.; Reynolds, J. R. *Synth. Met.* **2001**, *119*, 333. (b) Schwendeman, I.; Hickman, R.; Sönmez, G.; Schottland, P.; Zong, K.; Welsh, D. M.; Reynolds, J. R. *Chem. Mater.* **2002**, *14*, 3118. (c) Sönmez, G.; Schwendeman, I.; Schottland, P.; Zong, K.; Reynolds, J. R. *Macromolecules* **2003**, *36*, 639. (d) Cirpan, A.; Argun, A. A.; Grenier, C. R. G.; Reeves, B. D.; Reynolds, J. R. *J. Mater. Chem.* **2003**, *13*, 2422. (e) Sönmez, G.; Meng, H.; Wudl, F. *Chem. Mater.* **2004**, *16*, 574. (f) Thomas, C. A.; Zong, K.; Abboud, K. A.; Steel, P. J.; Reynolds, J. R. *J. Am. Chem. Soc.* **2004**, *126*, 16440. (g) Unur, E.; Jung, J.-H.; Mortimer, R. J.; Reynolds, J. R. *Chem. Mater.* **2008**, *20*, 2328. (h) Beaujuge, P. M.; Ellinger, S.; Reynolds, J. R. *Adv. Mater.* **2008**, *20*, 2772. (i) Beaujuge, P. M.; Ellinger, S.; Reynolds, J. R. *Nat. Mater.* **2008**, *7*, 795.

(11) Avendaño, E.; Azens, A.; Niklasson, G. A.; Granqvist, C. G. *Sol. Energy Mater. Sol. Cells* **2004**, *84*, 337.

(12) Mortimer, R. J.; Reynolds, J. R. *J. Mater. Chem.* **2005**, *15*, 2226.

(13) Mortimer, R. J.; Reynolds, J. R. *Displays* **2008**, *29*, 424.

(14) Reeves, B. D.; Grenier, C. R. G.; Argun, A. A.; Cirpan, A.; McCarley, T. D.; Reynolds, J. R. *Macromolecules* **2004**, *37*, 7559.

(15) Marcus, R. T. In *Color for Science, Art, and Technology*; Nassau, K., Ed.; Elsevier: Amsterdam, The Netherlands, 1998; pp 31−96.

AM900431Z